



Section 4

A neural model of saccadic eye movement control explains
task-specific adaptation

Gregory Gancarz, Stephen Grossberg *

Department of Cognitive and Neural Systems and Center for Adaptive Systems, Boston University, 677 Beacon Street, Boston MA 02215 USA

Received 16 July 1998; received in revised form 28 January 1999

Abstract

Multiple brain learning sites are needed to calibrate the accuracy of saccadic eye movements. This is true because saccades can be made reactively to visual cues, attentively to visual or auditory cues, or planned in response to memory cues using visual, parietal, and prefrontal cortex, as well as superior colliculus, cerebellum, and reticular formation. The organization of these sites can be probed by displacing a visual target during a saccade. The resulting adaptation typically shows incomplete and asymmetric transfer between different tasks. A neural model of saccadic system learning is developed to explain these data, as well as data about saccadic coordinate changes. © 1999 Elsevier Science Ltd. All rights reserved.

Keywords: Learning sites; Saccadic eye movement; Visual target; Neural model

1. Introduction

Saccades are rapid, ballistic eye movements which can be triggered by a variety of cues, including visual, auditory and planned cues. A key question is how multiple sources of saccadic commands are integrated. This integration requires learning. For example, auditory cues are initially represented in head-centered coordinates, because the ears are fixed in the head, whereas visual cues are initially represented in retinal coordinates, and the eyes move in the head. On the other hand, saccadic eye movements are often controlled by motor error coordinates, which represent the movement required to fixate the target (Mays & Sparks, 1980). These several coordinate systems are consistently mapped onto one another through a learning process.

1.1. Gain learning and map learning

There are at least two key types of saccadic learning: gain learning and map learning. Gain learning is pro-

posed to take place in the cerebellum (Grossberg, 1969; Marr, 1969; Albus, 1971; Fujita, 1982; Ito, 1984; Grossberg & Kuperstein, 1986; Dean, Mayhew & Langdon, 1994; Fiala, Grossberg & Bullock, 1996; Grossberg & Merrill, 1996; Houk, Buckingham & Barto, 1996), where it uses visual error signals due to incorrect saccades to adaptively tune the total input amplitude that reaches the saccade generator in the reticular formation, and in this manner keeps saccades accurate as eye muscles and other body parameters change. Gain learning is specific to amplitude, direction, and task (Wolf, Deubel & Hauske, 1984). For example, adapting the amplitude of 8° saccades has little effect on the amplitude of 2° saccades (Albano, 1996). Map learning allows the intermodal mixing of signals. For example, map learning allows visual cues, which are coded in a retinotopic coordinate system, to work together with auditory cues, which are coded in a head-centered coordinate system, to control saccadic movement parameters that are coded in a motor error coordinate system. Map learning can occur in several parts of the brain that are implicated in saccadic control, including the posterior parietal cortex, prefrontal cortex, and superior colliculus (Grossberg & Kuperstein, 1986; Zipser & Andersen, 1988; Grossberg, Roberts, Aguilar & Bullock, 1997).

* Corresponding author. Tel.: +1-617-3537857; fax: +1-617-3537755.

E-mail address: steve@cns.bu.edu (S. Grossberg)

1.2. Step task

A number of researchers have studied saccadic learning, and this work provides a powerful probe of the saccadic control circuits (Fitzgibbon, Goldberg & Segraves, 1986; Frens & van Opstal, 1994; Deubel, 1995; Melis & Van Gisbergen, 1996; Deubel, 1998). These studies implicate the superior colliculus (SC), parietal cortex (PC), frontal cortex (FC), and the cerebellum (CBLM) in such saccadic control. Many of these studies used the target displacement paradigm (McLaughlin, 1967; Hallett & Lightstone, 1976). Fig. 1A shows the step version of this paradigm.

The eye's position, shown by the dotted line, initially foveates a fixation point, shown by the dashed line. When the fixation point is turned off, a target appears, shown by the solid line in Fig. 1A. The subject's task is to saccade to this target. Before the saccade terminates, the eye tracking computer detects the saccade and displaces the target by a small amount. The subject is not consciously aware of the displacement due to saccadic suppression (Bridgeman, Hendry & Stark, 1975; Shioiri & Cavanagh, 1989; Li & Matin, 1997), and since the displacement is small. However, the saccadic system detects the shift, and the saccade amplitude slowly adapts to anticipate the target displacement. A typical adaptation profile is shown in Fig. 1B. The amplitude of the saccade is gradually reduced or lengthened over trials to foveate the displaced target. Less than 200 trials are typically necessary before adaptation is complete in humans (Deubel, 1995), and typically 400 are necessary in monkey (Fitzgibbon et al., 1986; Melis & Van Gisbergen, 1996). Following adaptation, if the target is no longer displaced, the learning extinguishes.

1.3. Electrical and memory tasks

Other versions of the target displacement paradigm also result in saccadic adaptation (Deubel, 1995, 1998). These tasks are shown in Fig. 2. In the electrical task (Fig. 2A), the subject initially views a fixation point. After the fixation point is extinguished, an electrical pulse is delivered to the superior colliculus, resulting in a saccade.

If a visual target is then shown slightly displaced from the endpoint of the saccade, adaptation occurs. In the memory task (Fig. 2B), a target is briefly flashed. Once the fixation point is extinguished, the subject is required to saccade to where the target was located. Thus, the memory task requires the subject to store the target position after the flash terminates. During the saccade, the target is reilluminated, but in a displaced location.

1.4. Overlap and scanning tasks

In the overlap task (Fig. 2C) the target and fixation point are on simultaneously. The subject is only allowed to perform the saccade when the fixation point disappears. By varying the amount of time the target and fixation point are simultaneously on, the experimenter can control the preparation the subject has before making a saccade. In the scanning task (Fig. 2D), the subject is required to sequentially foveate a number of letters (Deubel, 1995, 1998). After each saccade, the entire display is shifted slightly. This also results in saccadic adaptation.

1.5. Task-specific adaptation

One of the most interesting things about saccadic adaptation is that if one task type is adapted, this learning does not necessarily transfer to other task types (Fitzgibbon et al., 1986; Erkelens & Hulleman, 1993; Edelman & Goldberg, 1994; Frens & van Opstal, 1994; Deubel, 1995; Edelman & Goldberg, 1995; Fujita, Amagai & Minakawa, 1995; Fuchs, Reiner & Pong, 1996; Melis & Van Gisbergen, 1996; Deubel, 1998). For example, Fitzgibbon et al. (1986) and Melis and Van Gisbergen (1996) found that step task adaptation does not transfer to saccades evoked by electrical stimulation of the SC in monkey. However, electrical task adaptation resulted in 32% learning transfer to the step task (Melis & Van Gisbergen, 1996). The transfer between the step and electrical tasks is asymmetric, and incomplete. Human adaptation data also reveal asymmetries (Deubel, 1995). These data suggest that multiple sites exist at which saccadic adaptation occurs.

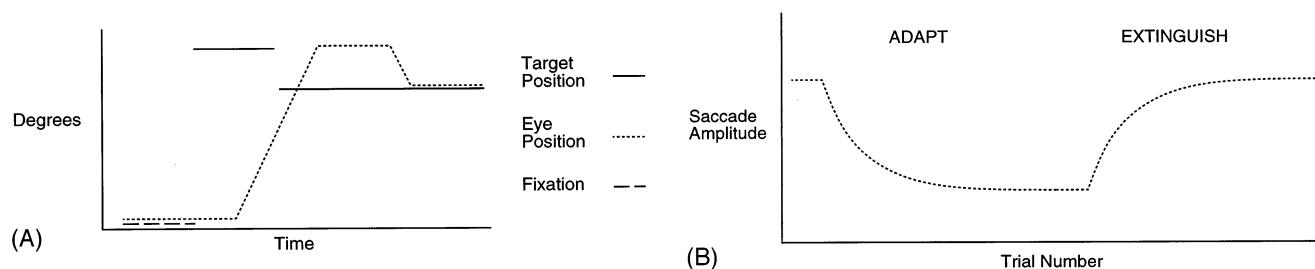


Fig. 1. (A) Step task. Solid line represents the target position as a function of time. Dotted line shows eye position, while the dashed line shows the fixation point. Target is displaced during saccade. (B) Typical saccadic adaptation profile in the target displacement task. Target is displaced during the adapt phase. Target is no longer displaced during the extinguish phase.

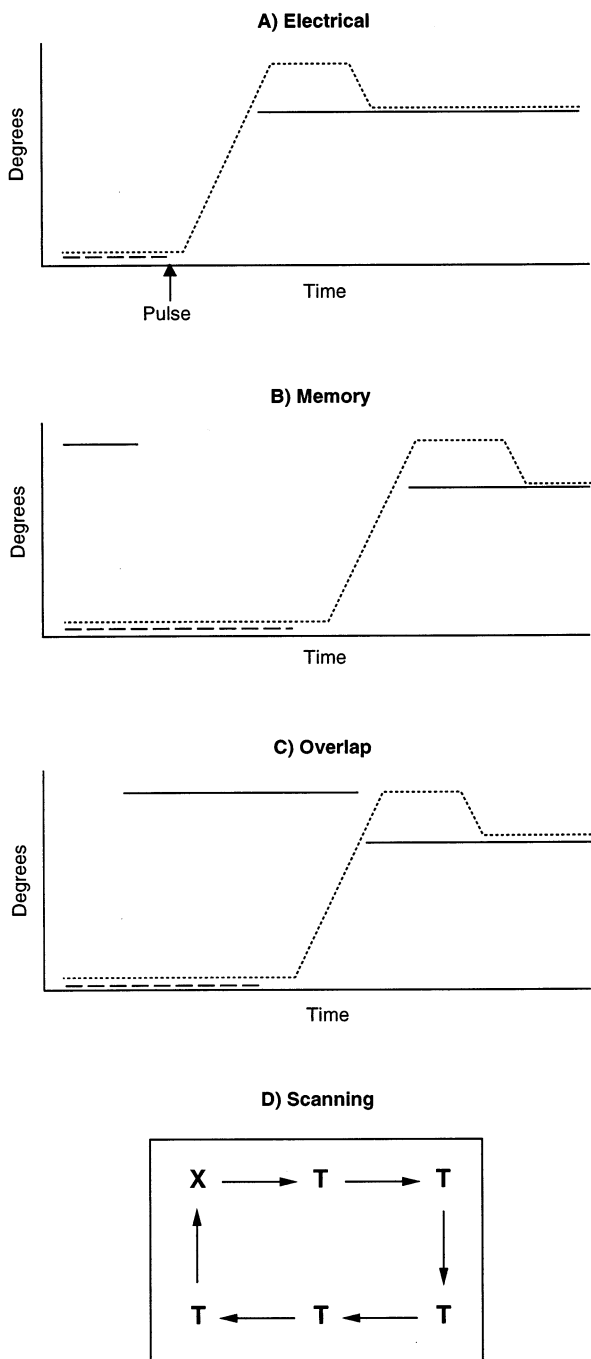


Fig. 2. Other target displacement tasks which result in saccadic adaptation. (A) Electrical task. (B) Memory task. (C) Overlap task. (D) Scanning task.

Why might such task-specific adaptation occur? It is well known that a large number of brain areas are involved in saccadic control. Some of these areas are more active in certain tasks than in other tasks. For example, the frontal eye fields (FEF) are primarily involved in planned eye movements (Burman & Segraves, 1994; Henik, Rafal & Rhodes, 1994). Further, there is multimodal convergence of visual, auditory, and planned signals on the SC and the paramedian

pontine reticular formation (PPRF) (Meredith & Stein, 1986). Thus there is likely varying amount of signal reaching the SC and PPRF depending on task. This paper presents a model that explains the task-specific adaptation data as a manifestation of the adaptive mechanisms which allow visually reactive, visually attentive, auditory, and planned saccades to all be made accurately, even though they are controlled by different combinations of brain regions. Some of this work has been briefly reported in Gancarz and Grossberg (1997, 1998a).

2. Methods

2.1. Reactive, attentive, and planned movement processing streams

The starting point of the present work is the SACCART model of how a multimodal movement map is learned in the SC (Grossberg et al., 1997). A simplified schematic diagram of the SACCART model is shown in Fig. 3A. The model simulates how visually reactive, visual and auditory attentive, and planned saccadic target positions become aligned through learning and compete to generate a movement command. This occurs by learning a transformation between attentive and planned head-centered representations and a motor error target representation in the deeper layers of the SC. The model provides functional roles for SC burst, buildup, and fixation cell types (Munoz & Wurtz, 1995a,b; Munoz, Waitzman & Wurtz, 1996). The burst cells or peak decay (PD) layer generate teaching signals

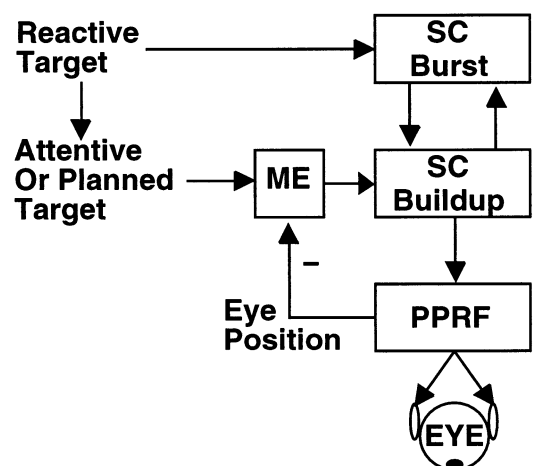


Fig. 3. (A) Simplified diagram of the SACCART model. (B) The extended model contains three processing streams: reactive, attentive, and planned. Motor error (ME), paramedian pontine reticular formation (PPRF), visual cortex (VC), posterior parietal cortex (PPC), prefrontal cortex (PFC), frontal eye fields (FEF), superior colliculus (SC), paramedian pontine reticular formation (PPRF).

to the buildup cell or spreading wave (SW) layer. The spreading wave layer displays a spreading wave of neural activity as a result of the process which renders the head-centered and motor error coordinates dimensionally consistent. The SACCART model simulated data about burst and buildup cell responses in visual, overlap, memory, gap, and multimodal saccade tasks (Meredith & Stein, 1986; Munoz & Wurtz, 1995a).

The SACCART model did not integrate the SC with the saccade generator that exists in the paramedian pontine reticular formation (PPRF), the gain learning circuits that occur in the cerebellum (CBLM), or the map learning mechanisms within the attentive and working memory circuits of the parietal (PPC) and prefrontal cortex (PFC), although the model did incorporate attentive and planned inputs to the SC. The present article extends the SACCART model to explicitly include these areas and their saccade-relevant adaptive processes. Simulations show that the extended model's mechanisms can explain the rather complex pattern of asymmetric and incomplete task-specific saccadic adaptation data, as well as additional data about vector saccades evoked by electrical stimulation of the SC and goal-oriented saccades evoked by electrical stimulation of the dorsomedial frontal cortex.

The extended model has three processing streams: a reactive stream, an attentive stream, and a planned stream, as shown in Fig. 4A. The streams have different latencies. The reactive stream is primarily involved in saccades made to flashing lights. The reactive stream has the shortest latency of the three streams as it is mediated, in part, through the direct connections between the retina and the superior colliculus. The reactive stream is proposed to be the means whereby very young children can make saccades to changing visual cues. The visual errors generated in this way are corrected by cerebellar learning until reactive saccades are accurate (Grossberg & Kuperstein, 1986). The attentive stream is mediated through visual and parietal cortex and has a medium latency (Mountcastle, Anderson & Motter, 1981; Robinson, Bushnell & Goldberg, 1981; Posner, Walker, Friedrich & Rafal, 1987; Steinmetz & Constantinidis, 1995). In the model, the attentive stream controls saccades made in a step task. The planned stream is mediated through prefrontal cortex and the frontal eye fields whose working memory capabilities aid in saccadic planning (Zingale & Kowler 1987; Goldman-Rakic, 1990; Wilson, O'Scalaidhe & Goldman-Rakic, 1993; Goldman-Rakic, 1995; Fuster, 1996). The planned stream has the longest latency since its signals must pass all the way through frontal cortex. The planned stream controls long latency saccades such as those made in overlap and memory

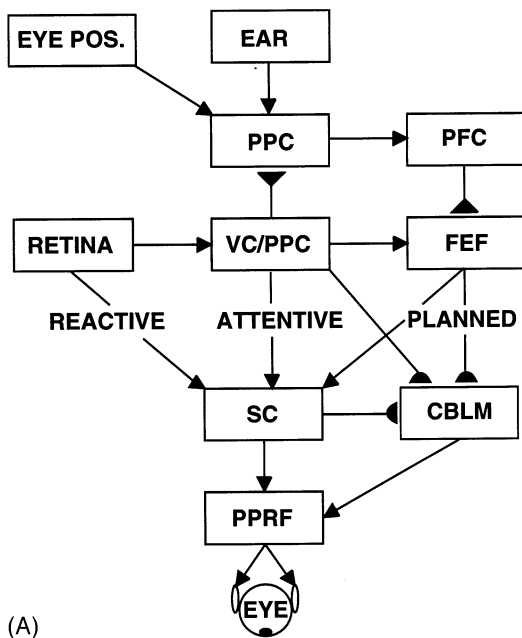
tasks. The model proposes that learning is distributed across these pathways in a way that can explain the task-specific adaptation data.

The three streams converge on the SC, where a target is chosen (Schiller, True & Conway, 1979; Mays & Sparks, 1980; Grossberg et al., 1997). The activity of each stream depends on a number of factors such as saccade latency and task type, much as the frontal eye field has the longest latency and is primarily involved in planned eye movements (Segraves & Park, 1993). Thus, the total amount of signal reaching the SC may depend upon the task. As a result of this task-specific variation in total input to the SC, as well as to other saccade-controlling brain regions (Munoz & Wurtz, 1995a,b; Edelman & Goldberg, 1998), it would be possible for each task type to generate saccades of different amplitude and/or direction in response to a target at a fixed position. In order to accurately calibrate saccades in all task types, each stream needs to be able to adaptively compensate for this type of variability.

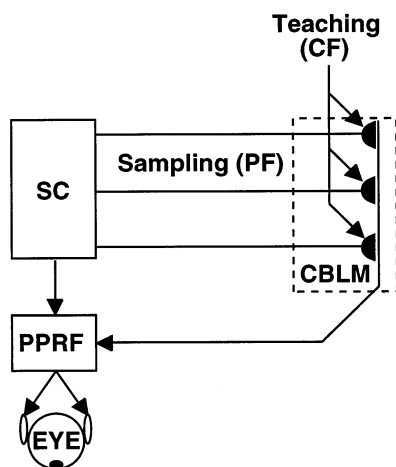
As noted above, two types of learning occur in the model: gain learning and map learning. As shown in Fig. 4A, gain learning (represented by the half circles) is proposed to occur in the cerebellum, whereas map learning can occur between several different brain regions. As shown by the triangles, model map learning occurs in the PPC and between the PFC and the FEF. Note that the model stage labeled VC/PPC is a retinotopic map, like those found both in visual as well as parietal cortex (Barash, Bracewell, Fogassi, Gnadt & Andersen, 1991a; Schall, Morel, King & Bullier, 1995). The model stage labeled PPC codes targets in head-centered coordinates, and map learning occurs between these two stages (Grossberg & Kuperstein, 1986; Zipser & Andersen, 1988). It is possible that both of these representation coexist in the PPC, or involve visual cortex. To illustrate the site of map learning, the PPC is broken into two boxes in the diagram. Each type of learning will now be discussed in detail.

2.2. Cerebellar gain learning

Each of the model streams participates in gain learning in the cerebellum. Gain learning keeps saccades accurate as eye muscles and other body parameters change, and is specific to amplitude, direction, and task. The model SC, VC/PPC, and FEF each send sampling signals to the cerebellum. These signals can reach the cerebellum through known connections with the nucleus reticularis tegmenti pontis (NRTP) and the pontine nuclei (Crandall & Keller, 1985; Thielert & Thier, 1993). Experimental studies have implicated the cerebellum in motor learning (Eccles, 1979; Perrett, Ruiz & Mauk, 1993), and a num-



(A)



(B)

Fig. 4. (A) Model learning sites. Map learning sites shown by the triangles, gain learning by the half circles. (B) Gain learning. Sampling signals from each of the model streams (only reactive shown here) send sampling signals mediated by parallel fibers (PF) to the cerebellum (CBLM). The sampling signals are multiplied by adaptive weights. If a post-saccadic error exists, the cerebellar weights are modified by a visual teaching signal which is mediated by climbing fibers (CF). Superior colliculus (SC), paramedian pontine reticular formation (PPRF).

number of models of such learning have been proposed (Grossberg, 1969; Marr, 1969; Albus, 1971; Fujita, 1982; Grossberg & Kuperstein, 1986; Dean et al., 1994; Fiala et al., 1996; Grossberg & Merrill, 1996; Houk et al., 1996).

Fig. 4B shows how gain learning operates in the present model. Each location in the SC map sends sampling signals to the CBLM via mossy fibers. These sampling signals are multiplied by adaptive weights. The weighted sampling signals each input to the paramedian pontine reticular formation (PPRF), which contains the saccade generator (Raybourn & Keller, 1977; Noda,

Sugita & Ikeda, 1990). By contributing more or less signal to the PPRF, the adaptive weights can modify the amplitude of a saccade. If a saccade is inaccurate, a visual error teaching signal adjusts the adaptive weights to reduce the saccadic error (Grossberg & Kuperstein, 1986). This teaching signal is proposed to be carried by cerebellar climbing fibers, which originate in the inferior olive (IO) (Ojakangas & Ebner, 1992). The IO likely receives the error signal from the SC to IO connection (Ito, 1984).

In addition to the SC, the model VC/PPC and the model FEF also send sampling signals to the cerebellum (Crandall & Keller, 1985; Thielert & Thier, 1993), and each stream's adaptive weights are taught using the same teaching signal from the IO. Learning in the various task types shown in Fig. 2 is mediated by different streams in the model. Electrical trial adaptation modifies the reactive (SC) cerebellar weights. Step trial learning involves the attentive stream's weights (VC/PPC). Finally, overlap and scanning adaptation primarily modifies the planned stream's (FEF) cerebellar weights. In the present model, the primary determinants of which areas are involved in a task is whether a target is visually present at the time of the saccade, as well as the latency of the saccade. For example, during a visually-guided task, it is known that both the superior colliculus as well as the visual and parietal cortices become active (Schall, 1991), and this also occurs in the model. On the other hand, when a short-latency visually-guided saccade is produced, the model's PFC is not significantly active since the target signal must pass through numerous stages to reach the PFC.

A hypothesis of the current model is that the sampling signals from the three streams compete through mutual inhibition and that this competition typically favors the attentive and planned streams. This competition may occur in the cerebellum (Eccles, Ito & Szentagotai, 1967), or in the nucleus reticularis tegmenti pontis (NRTP) or pontine nuclei, which are way-stations through which sampling signals pass on their way to the CBLM (Crandall & Keller, 1985; Schall, 1991; Gamlin & Clarke, 1995). Essentially, this competition realizes a hierarchy of control between the model streams. The planned stream sampling signals can override the attentive streams signals, and both of these can override the reactive stream sampling signals. In this manner, if one area's weights are modified (such as those of the SC), this learning may not disrupt the calibration of the other streams.

2.3. Head map learning

Map learning allows the intermodal mixing of signals. For example, a parietal head-centered map (An-

dersen, Essick & Siegel, 1985; Stricanne, Andersen & Mazzoni, 1996), which codes targets in terms of their position with respect to the head, allows these visual cues to cooperate or compete for attention with auditory cues, which are coded directly in head-centered coordinates. A head-centered target representation is also useful for storing several sequential target positions in short-term memory, since if a saccade to a stored target position is inaccurate, a head-centered target position does not need to be updated or recoded. If the target position were stored retinally and updated after each intervening saccade, as proposed by Goldberg and his colleagues (Duhamel, Colby & Goldberg, 1992; Colby, Duhamel & Goldberg, 1995), one would expect a substantial accumulation of error as the number of intervening saccades was increased. However, Karn, Moller and Hayhoe (1997) found only a slight increase in error when subjects performed saccades to memorized targets flashed before a number of intervening saccades were made. They interpreted their data as supporting a head-centered target representation, since to account for their results with an updating mechanism would require an unlikely degree of precision in the eye position signal. Such a head-centered representation may exist in the parietal cortex, as well as the dorsomedial frontal cortex (DMFC), where electrical stimulation results in goal directed saccades (Mann, Thau & Schiller, 1988; Lee & Tehovnik, 1995) that terminate in a particular region of craniotopic space, irrespective of the initial eye position, as we simulate below.

The head-centered representation of target position is formed in the model by combining retinal target positions with initial eye positions. Signals from the retinotopic visual map are multiplied by adaptive weights. The weighted retinal input, when combined with an eye position signal, forms a head-centered vector representation in the PPC (Fig. 4A). The adaptive weights between the retinal map and the PPC head-centered representation are learned in the model by using a corollary discharge of eye position, after a saccade occurs, as a teaching signal. This teaching signal adjusts the adaptive weights until there is no further error between the head-centered target representation and the actually realized eye position (Grossberg & Kuperstein, 1986; Grossberg, Guenther, Bullock & Greve, 1993). Eye position after an accurate saccade can be used as a teaching signal with which to learn the head-centered target because such a saccade foveates the target. In this way, the visual error signals that make reactive saccades accurate may be used to learn an accurate head-centered parietal map.

2.4. Working memory target storage

Attended targets in the PPC are stored in the model

PFC. This is consistent with findings suggesting that the dorsolateral prefrontal cortex (PFC) is involved in working memory storage of targets (Goldman-Rakic, 1990; Wilson et al., 1993; Goldman-Rakic, 1995). Like the model PPC, the model PFC stores targets in a head-centered representation. However, unlike the PPC, model PFC cells can continue to store a target after another target is attended by the model, and take longer to be activated. To trigger a saccade, targets that are stored in the PFC are transformed into a motor-error map so they can compete with reactive and attentive targets in the SC of the model. This transformation is learned in the model by using a corollary discharge of eye position to teach the map weights, after an accurate saccade occurs (Grossberg et al., 1997). Grossberg et al. (1997) have shown how the transformation from a head-centered target to a motor-error map results in a spreading wave of activity, as has been found among the buildup cells in the deeper layers of the SC (Munoz & Wurtz, 1995b). The transformation from the head-centered planned target to a motor-error map allows reactive, attentive, and planned input sources to compete in a common coordinate system in the SC to select a winning target location (Grossberg et al., 1997).

3. Results

The model is described by differential equations representing cell activities, as given in the Appendix A. The following simulations illustrate that the model can explain many aspects of the saccadic adaptation data.

3.1. Transfer between electrical and step tasks

Fitzgibbon et al. (1986) adapted a monkey's saccades in a step task and, interspersed with these step trials, electrically stimulated the SC (electrical trials). The results from this experiment are shown in Fig. 5A, where triangles denote the amplitudes of electrically elicited saccades and dots the step trial amplitudes. For the first few trials, the amplitudes of step and electrical saccades were the same. Soon, however, the amplitude of step saccades decreased due to the target displacement. The step trial adaptation does not affect the amplitudes of electrical saccades, as illustrated by the central group of triangles in the data plot. During the last few hundred trials, the target was no longer displaced, and the learning was extinguished.

A simulation of the Fitzgibbon et al. (1986) experiment is summarized in Fig. 5B, which replicates the time course of adaptation, as well as the lack of adaptation transfer between the step and electrical tasks. The model first performed a single electrically elicited trial in which a caudal location of the model SC was stimulated. The amplitude of the saccade for this task is

shown by the leftmost triangular point. After the first electrical trial, a number of step trials (dots) were performed in which the target was displaced by a fixed amount from the initial target position, which caused saccade size to decrease gradually as cerebellar learning occurs. Then, another electrical trial was performed. Note that the amplitude of the electrical saccade did not decrease. No transfer of learning occurred from the step to the electrical task. Next, the model again performed a number of step tasks, this time without target displacement, so that learning is extinguished. Finally,

another electrical trial was performed. The shape of the adaptation profile in the simulation, as well as the lack of learning transfer, matches that from the experiment by Fitzgibbon et al. (1986).

Fig. 5C shows the reverse case: electrical trial adaptation and step tests. In the electrical adaptation trials, a caudal location of the model SC was stimulated to simulate electrical stimulation of the SC. At the end of the elicited saccade, a visual target was presented at a fixed position which was slightly displaced from the unadapted electrically elicited saccade endpoint. This resulted in adaptation, such that the amplitude of the electrically elicited saccade changed to land closer to the visual target. Step trials were interspersed with the electrical adapt trials. There was little transfer of learning between the tasks, in agreement with experimental data (Melis & Van Gisbergen, 1996).

The amount of adaptation transfer between two tasks (adapt task A, test task B) can be defined by:

$$\% \text{ transfer} = \frac{\Delta B}{\Delta A} \quad (1)$$

where ΔA is the change in saccade amplitude for task A (the adapted task in which the target is displaced) and ΔB is the change in saccade amplitude for task B after adaptation has occurred in task A. If target displacement during task A trials causes task B trials to change in amplitude by a similar amount, then 100% transfer has occurred. The amount of transfer from Fig. 5 is shown in Table 1, along with experimental data in monkey for comparison. In the boxes, the left number is experimental data (Melis & Van Gisbergen, 1996), and the right number the simulation result.

The low levels of learned transfer between the step and electrical tasks occurs in the model because the tasks are controlled by different model streams. In the electrical task, only the later stages of the visually reactive stream are activated, since only the SC is stimulated and no visual target is presented. The SC-activated cerebellar weights are thus read out during such a saccade (Crandall & Keller, 1985; Thielert & Thier, 1993). As a result, if the target is displaced, these reactive weight strengths change to adjust the saccade. No learning occurs in the attentive or planned cerebellar weights because those streams are not activated by electrical stimulation of the SC. There is some learning transfer from electrical adaptation to step trials in the model (17% for the present choice of parameters), since in the step task, a visual target is present, so both the attentive stream and the reactive stream are activated via the VC and PPC. During a step saccade, the attentive stream cerebellar weights tend to dominate the saccade amplitude, since attentive stream sampling signals override reactive stream sampling signals due to a mutual competition which favors the attentive stream. However, since the SC cells are also fully active, some

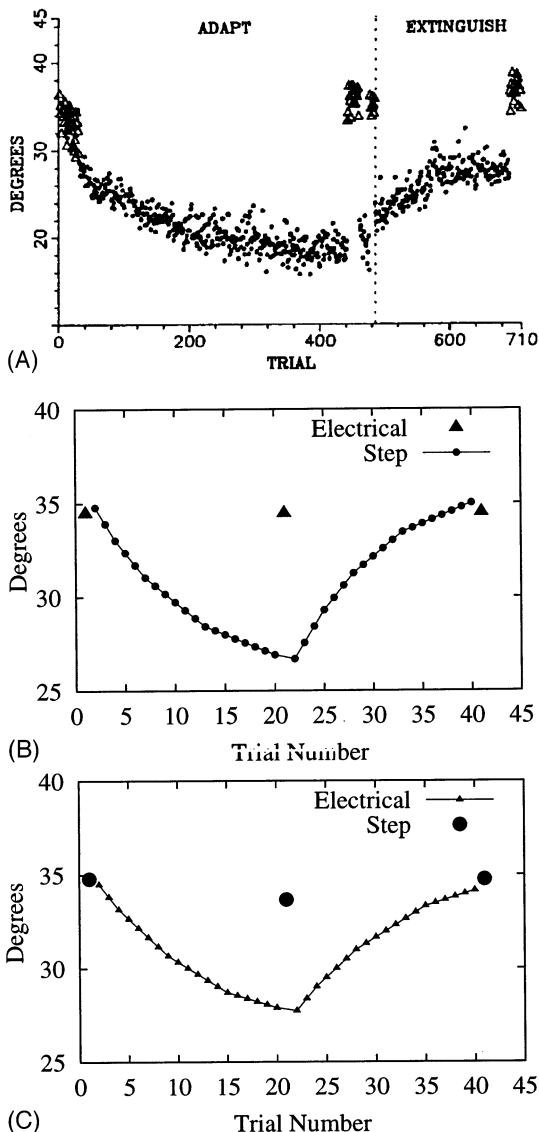


Fig. 5. (A) Results from experiment in which step trials were adapted (dots), and electrical trials were tested (triangles). [Reprinted from Fitzgibbon et al. (1986) with permission]. (B) Simulation of step adaptation data (dots), with electrical trials interspersed (triangles). Like the experimental data, model step task adaptation does not affect saccades evoked by electrical stimulation of the superior colliculus. (C) Simulation in which electrical trials were adapted (triangles), with step trials interspersed (dots). There is very little learning transfer from the electrical to the step trials.

Table 1
Adaptation results summary^a

Test	Electric (%)		Step (%)		Overlap (%)		Scanning (%)		Memory (%)	
<i>Adapt</i>										
Electric (%)			32	17	–	1	–	3	–	27
Step (%)	0	0			9	11	11	29	2	10
Overlap (%)	–	7	–	16			–	98	–	86
Scanning (%)	–	28	37	37	76	91			90	92
Memory (%)	–	1	17	1	7	12	9	12		

^a Comparing experimental (left) and simulated (right) learning transfer across a variety of tasks. Experimental entries where data do not exist are labeled with a –, and the corresponding simulated values are model predictions. Monkey data (step to electrical, and electrical to step) from Melis and Van Gisbergen (1996). Human data from Deubel (1998).

reactive sampling activity survives the competition, and thus influences the saccade generator, resulting in partial learning transfer.

Based on the above, one might expect that some transfer to electrical test trials may occur as a result of step adaptation trials. However, it is known that SC burst cell activity decays with current gaze error (Munoz & Wurtz, 1995a), while VC and PPC activity tends to persist well after saccade termination (Barash, Bracewell, Fogassi, Gnadt & Andersen, 1991b). Model SC burst cell activity also decays with current gaze error (Grossberg et al., 1997). Thus, during a step trial saccade, both the reactive and attentive streams can influence the saccade. As the saccade progresses, however, the reactive stream becomes less and less active, since the SC burst cell activity decays. By the time the visual teaching signal arrives, only the attentive sampling signals are present. For this reason, only the attentive weights learn during a step adaptation trial, and there is no learning transfer from step to electric trials. In summary, during an electrical trial, learning occurs only in the reactive cerebellar weights, whereas during a step trial, learning occurs only in the attentive weights.

3.2. Transfer between step and overlap tasks: role of saccade latency

Deubel (1995, 1998) showed that the amount of transfer from an adapted step task to an overlap task depends on the saccade delay, as shown in Fig. 6A. Saccade delay is the amount of time between peripheral target appearance and saccade onset. The saccade delay was varied in the overlap task by changing when the fixation point disappeared. Open circles in the figure show overlap saccade amplitude as a function of saccade delay before step adaptation trials were performed. Filled circles show overlap amplitude as a function of delay after step adaptation trials. These step adaptation trials decreased saccade amplitude. At short saccade delays, the overlap amplitude decreased sub-

stantially due to the step adaptation trials. There is nearly complete learning transfer from the adapted step trials to the overlap trials. However, at larger delays, step adaptation has only had a small effect on overlap trial saccade amplitude.

Fig. 6B shows the results from a simulation of Deubel's experiment. The model first performed a number of overlap trials in which the fixation point offset time was varied from 0 to 750 ms. This resulted in a variety of saccade delays. The saccade amplitude from these trials is plotted by the line labeled pre-adapt in the Figure. Then the model performed a number of step adaptation trials in which the target was displaced and

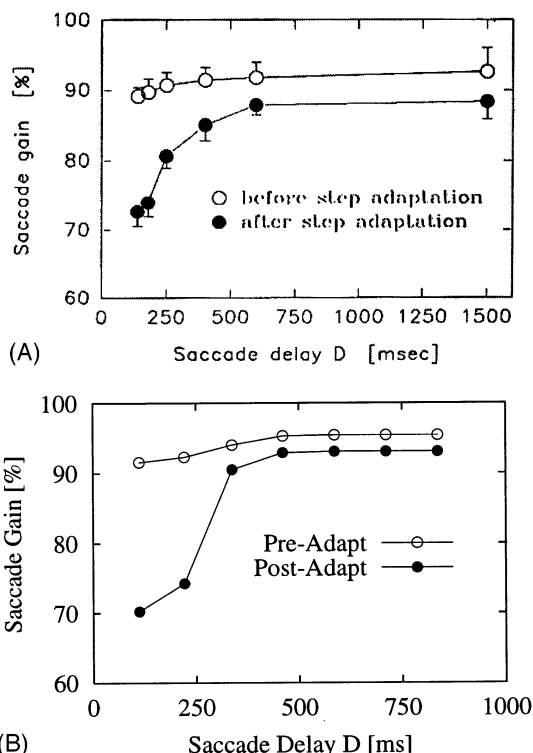


Fig. 6. (A) Learning transfer from step task to overlap task depends on saccade delay. [Reprinted from Deubel (1997) with permission.] (B) Simulation of saccade delay effect.

adaptation occurred. These trials are not shown in the Figure. Finally, the model was again tested in an overlap task, and the fixation point offset time varied. These results are plotted by the postadapt line. With short saccade delays, the step adaptation transfers to the overlap trials. However, with long saccade delays (ample preparation), there is little transfer. Thus, the amount of transfer in the model depends on saccade delay, as in the human data.

The dependence of learning transfer on saccade delay occurs in the model as follows. During step trials, or overlap trials in which the fixation point goes off rapidly (short saccade delay), the attentive gains from the visual and parietal cortex are read out, and it is these weights which learn when the target is displaced. Thus, step trials and overlap trials with short saccade delays share a common set of cerebellar gains. This results in step adaptation transferring to short delay overlap trials. In the step and short delay overlap trials, the planned stream does not have sufficient time to become activated (since its signals must pass all the way through prefrontal cortex), and thus the planned stream cerebellar weights are unchanged by step trial adaptation. As the saccade delay is increased, the planned stream begins to affect the saccade. The planned stream sampling signals compete with the attentive stream sampling signals. As the planned stream becomes very active, its sampling signals dominate, as the planned stream occupies the highest position in the stream hierarchy of control. The planned stream's sampling signals are favored over the attentive stream's sampling signals in the sampling signal competition, just as the attentive stream's sampling signals override those of the reactive stream. Thus, with long saccade delays, the planned stream cerebellar weights are read out. These weights were unchanged by the step trial target displacement. For this reason, overlap trials with long saccade delays are relatively unaffected by step trial adaptation.

3.3. *Transfer between scanning and memory tasks: role of map learning*

As discussed earlier, a head map uses the intermodal mixing of signals to learn a coordinate transformation. It will now be shown how it can, as a result, also lead to an adaptation asymmetry between scanning and memory tasks, as found in the data (Table 1): Scanning adaptation transfers nearly completely to memory trials, but memory adaptation does not transfer to scanning trials (Deubel, 1995, 1998).

As shown in Fig. 4A, model map learning occurs in the PPC as well as between the PFC and the FEF. The PPC learns to code targets in a head-centered coordinate system, and the PFC to FEF weights learn to recode a head map into a motor error vector. This

learning is needed to render targets in the model PPC and PFC, which are coded in a head-centered coordinate system, dimensionally consistent with the FEF and the SC, which code targets in a motor-error coordinate system (Andersen et al., 1985; Grossberg & Kuperstein, 1986; Zipser & Andersen, 1988; Kurylo & Skavenski, 1991).

It is important to consider what effect target displacement has on the various map weights of the model. Target displacement in the various tasks modifies the PPC head map weights, since these weights are learned using eye position after the primary saccade, and target displacement modifies this saccade amplitude. However, this reorganization of the internal target representation occurs slowly since the head map learning is parasitic to the gain learning in the cerebellum. By this we mean that because the head map is learned using final eye position after a saccade, until the saccade amplitude changes significantly, the head map does not change. Thus, much as the model head map can only be learned after reactive saccades have been rendered accurate by cerebellar learning, any head map reorganization depends on cerebellar gains changing the saccade amplitude. Also, since in the model the VC/PPC map holds one target at a time, after target displacement, the displaced target excites a new location in the VC/PPC map. This new target activity inhibits the old target representation, thus eliminating the head map sampling signal which serves as a substrate for learning. During electrical adaptation trials in which the SC is stimulated, there is no parietal head map reorganization since, in this type of trial, the VC/PPC map is not active.

What is the effect of target displacement on the weights read out of the PFC? Target displacement during a step trial or other short latency saccade has little effect on the PFC to FEF learned weights because the PFC does not have sufficient time to become activated due to the short saccadic latency during step tasks. However, in the scanning, overlap, and memory tasks, the target displacement does modify the learned weights between the PFC and the FEF. This occurs because the saccadic latency of those tasks is sufficient to allow the PFC to become active, and this mapping, like the head map, is learned using an eye position teaching signal that is registered after a saccade. As a result, after saccadic adaptation in the scanning and memory tasks, a target stored in the PFC activates a slightly different location in the FEF.

How do these processes influence the asymmetry in learning transfer between scanning and memory tasks? Target displacement in both the scanning and memory tasks modifies the target location read out of the PFC, as described above. However, in addition to connections from the PFC (Schall, 1991), the FEF is also known to receive input from extrastriate and parietal

cortical areas (Fischer & Boch, 1991; Schall et al., 1995); see Fig. 4A. Typically, the visual/attentive (VC/PPC) input and the memory (PFC) input to the FEF will be in agreement, and code the same amplitude saccade. However, after saccadic adaptation in a scanning or memory task, the model adaptive weights between the PFC and the FEF will have been modified, and thus the PFC will excite a slightly different location in the FEF from the direct visual input. The visual and attentive input from the model striate and extrastriate visual areas is, however, stronger than the memory (PFC) input to the FEF, and therefore overrides the modified memory signal.

Scanning adaptation transfers to memory trials in the model as follows. During the scanning adaptation trials, the map weights between the PFC and the FEF are modified. The PFC head map stores a target as a position of the eye in the head, and sends this information to the FEF. Scanning adaptation trials modify the location read out to the FEF such that the value sent is the location of the target in the head after the displacement (the target shift). During subsequent memory trials, the target eye location read out from memory (PFC) is the displaced target location. This means that scanning adaptation transfers to memory trials.

Memory adaptation does not transfer to scanning trials despite the fact that memory adaptation trials also modify the head weights between the PFC and the FEF. In subsequent scanning trials, the memory and visual inputs to the FEF are out of alignment. Since the visual/attentive inputs to the FEF in the model are stronger than the memory inputs, the unadapted saccade coded by the visual signal tends to dominate. Thus, memory adaptation does not transfer significantly to the scanning task. The direct connection from the retina to the SC also helps ensure that, when the memory and the visual representation of the target disagree, the saccade is made to the visual input.

The hypothesis that visual/attentive inputs dominate memory inputs to the FEF is consistent with the role of visual/attentive inputs as teaching signals for learning, and maintaining accurate calibration of, the mapping from the PFC head map to the FEF motor-error map. Since these visual/attentive teaching signals are likely to be more accurate than memory traces, they dominate the memory traces in the model.

These remarks hold for the case in which both vision and memory represent the same target locations. If the visually attended location represents a different location than the memory trace, then feedback connections from the PFC to the PPC may ensure that the planned target dominates, by changing the focus of attention in the PPC to the memorized location (Grossberg & Merrill, 1996). Such feedback connections were not included in the model as they were not needed to explain the present data.

These feedback connections are, however, conceptually important because they suggest how planned targets can dominate vision when recalibration is not required, even though vision can dominate memory traces when recalibration may be required. This hypothesis is consistent with the fact that the model's planned stream dominates the competition at the cerebellum, too, as was used to analyze the data in Fig. 6. The planned output to the cerebellum is derived from the model FEF, but only after visual/attentive and memory traces at the PPC and PFC have determined which FEF vector will be activated. Thus, although vision can instruct the PFC-to-FEF mapping, the planned stream dominates, other things being equal.

3.4. *Transfer summary*

Table 1 compares the simulation transfer results to experimental data for human and monkey in a variety of tasks (Melis & Van Gisbergen, 1996; Deubel, 1998). Possible differences between monkey and human saccadic adaptation data are reviewed in Section 4. Where experimental data exists, there is a qualitative match in gain transfer. Where there are not yet experimental data, the model makes testable predictions. For example, the model predicts that memory adaptation will not transfer to saccades elicited by electrical stimulation of the deeper SC layers. This occurs in the model since memory adaptation is mediated by the map weights between the PFC and the FEF, and does not modify the cerebellar gains which are read out during electrical stimulation of the SC. The model also predicts that electrical trial adaptation will only have a limited effect on overlap, scanning, and memory trials, since the attentive and planned cerebellar gains override the SC reactive cerebellar gains.

3.5. *Vector and goal-directed saccades*

The above explanations involve the transformation of saccade-generating data between retinotopic, head, and motor-error coordinates. Various other data are consistent with these model hypotheses. For example, when the SC or the FEF is electrically stimulated, vector-like saccades are produced in which the saccade direction and size are largely independent of the initial eye position (Robinson & Fuchs, 1969; Schiller & Stryker, 1972). Fig. 7A shows the results of four trials in which the SC of the model was electrically stimulated. The initial eye position was varied for each trial. However, the stimulation location, strength, and duration were all held constant. The amplitude and direction of each saccade is the same, showing that the electrical stimulation of the model SC evokes vector saccades. Stimulation of the model FEF produces similar results. Eventually, at more eccentric starting posi-

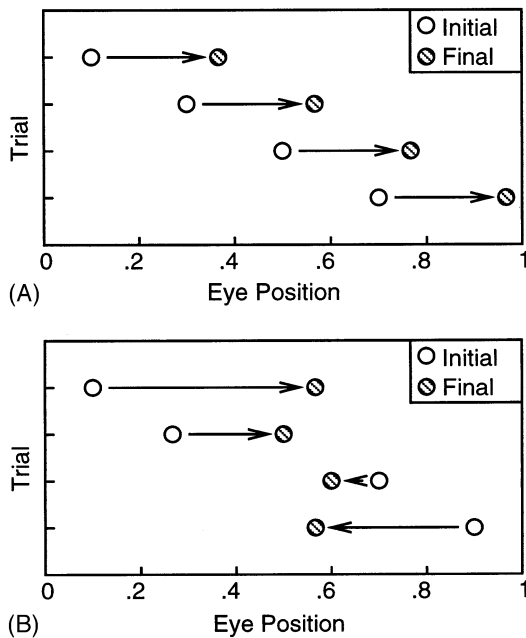


Fig. 7. (A) When saccades are evoked by electrical stimulation of the superior colliculus, saccade amplitude and direction do not depend on initial eye position (Schiller & Stryker, 1972). Model simulation in which model superior colliculus was stimulated from four different initial eye positions. Model saccades are of the same amplitude and direction. (B) Goal-directed saccades evoked by electrical stimulation of the dorsomedial frontal cortex tend to terminate in a particular region of craniotopic space (Tehovnik et al., 1994). Goal-directed saccades evoked by electrical stimulation of a single site in the model prefrontal cortex. Only initial eye position was varied. Each of the model saccades brings the eye to approximately the same position in the head.

tions, the saccades would become shorter, if only because of cell saturation and approach to the edge of the workspace.

When the dorsomedial frontal cortex (DMFC) is electrically simulated, goal-directed saccades are produced, which terminate in a particular region of craniotopic space, irrespective of the initial eye position, as shown in Fig. 7C (Mann et al., 1988; Tehovnik, Lee & Schiller, 1994; Lee & Tehovnik, 1995). Fig. 7B shows a simulation in which the model's PFC was electrically stimulated. Again, only the initial eye position was varied. Stimulation location, strength, and duration were held constant. When the PFC of the model is stimulated, saccades converge on a single region of space. Depending on initial eye position, saccades can be rightward, or leftward, as found in the data (Mann et al., 1988; Tehovnik et al., 1994). The model can explain these data because the model PFC codes targets in a head-centered coordinate system, and these targets get transformed into motor error coordinates by using eye position information, as discussed earlier. In the model results, goal-directed saccades converged only to an approximate region in space due to the limited number of cells in the model maps (coarse coding). In

the monkey results, it is likely that electrical stimulation does not accurately replicate typical cell activity distributions, so the coding under these conditions may also be coarse.

4. Discussion

4.1. Adaptive movement calibration by multiple processing streams

The simulations presented above show that the model can reproduce the saccadic adaptation transfer data, as well as data concerning vector and goal-directed saccades. The model suggests that these data are manifestations of multiple adaptive processing streams which allow the saccadic system to react rapidly to perceptually salient targets from several modalities, and still perform complex planned movements, without a loss of accuracy. The present model has three processing streams; reactive, attentive, and planned, that enable the brain to balance between the demands of momentary perceptual signals and more cognitive plans. The existence of three separately adaptable streams is suggested by anatomical and lesion data (Schiller & Sandell, 1983; Keating & Gooley, 1988a,b; Lynch, 1992), as well as by the adaptation data which show that electrical, step, and scanning tasks can be adapted relatively independently of one another (Deubel, 1995; Melis & Van Gisbergen, 1996; Deubel, 1998).

Correspondingly, each of the model streams participates in gain learning at the cerebellum. Each stream needs its own adaptable cerebellar gain weights because signals from a large number of saccade-related brain areas converge on the SC and the PPRF. Since some areas are more active in certain tasks than in others, the total movement signal reaching the SC and PPRF could change with task, even for saccadic targets of similar eccentricity. Saccade amplitude has been recently shown to depend on the activity and strength of collicular activity. For example, Stanford, Freedman and Sparks (1996) varied the frequency of electrical stimulation to the SC and found that the amplitude of a saccade evoked from a particular point on the SC is not only a function of stimulation location. Rather, the stereotypical saccade amplitude for a particular site is obtained only with sufficiently high stimulation frequency. Below this level, saccades of smaller amplitude are produced. The FEF can also bypass the SC through direct connections with the PPRF (Schnyder, Reisine, Hepp & Henn, 1985; Schlag-Rey, Schlag & Dassonville, 1992; Segraves, 1992). With the total amount of signal reaching the SC and PPRF being dependent on task, multiple sites of learning are needed to calibrate the total movement signal in each task type.

4.2. How do memory-guided saccades get calibrated?

One exception to adaptive independence are memory saccades. Deubel (1995, 1998) found that adaptation in a scanning task has a large effect on memory-guided saccades. Based on this data, Deubel (1998) suggested that memory-guided saccades utilize FEF connections to the saccade-generating circuits, and are thus affected by any changes in the FEF learned gains. Our present simulations support this view. Why might memory targets, which we believe are stored in the PFC, need to use the learned cerebellar gains of the FEF pathway? One possible reason for this is that in a natural memory task, unlike those typically performed in a lab, the target may not conveniently reappear after the saccade. Thus, in natural memory saccades, there may never be a visual teaching signal with which to accurately adapt memory saccades. For this reason, memory saccades may use the FEF, which is active in planned visually-guided saccades, and can thus be adaptively tuned by visual error signals.

The model FEF receives both visual/attentive signals from the VC/PPC stage, as well as memory-based signals from the PFC, and in this manner memory-based saccades can use the FEF's learned cerebellar gains. This architecture is directly supported by anatomical studies (Fischer & Boch, 1991; Schall, 1991; Anderson, 1995; Schall et al., 1995) and indirectly supported by the finding that memory-guided saccades are typically hypometric and slower than visually-guided saccades (White, Sparks & Stanford, 1994), as also occurs in the model. In long-latency visually-guided saccades, the FEF receives both visual/attentive input from the VC/PPC, as well as memory input from the PFC, since the latency is sufficient to activate the model PFC. However, in the memory condition, the VC/PPC input is absent, since the target is no longer visible. Thus, the FEF receives less input in the memory case than in the long-latency visually-guided case. We suggest that this is one reason why memory saccades are typically hypometric and of relatively low velocity.

The proposal that memory-guided saccades are mediated through the FEF is also consistent with the lesion data of Deng, Goldberg, Segraves and Ungerleider (1986). They found that monkeys with lesions of the FEF have severe deficits in the performance of saccades to memorized targets. This result is consistent with the present model since in the model, memory-guided saccades are mediated through the FEF. Thus, if the model FEF was lesioned, memory signals from the PFC may be unable to reach the SC and PPRF, and thus memory-guided saccades in the model would also show severe deficits.

In addition to the simulations presented in the Results section, the present model is also consistent with a variety of other data. Further support for the model

comes from the recent experiments of Brandt, Ploner, Meyer, Leistner and Villringer (1998). They found that magnetic stimulation over area 46 in the prefrontal cortex (PFC) impairs memory-guided saccades. Brandt et al. (1998) also found that stimulation over the posterior parietal cortex only impairs memory-guided saccades when applied within the sensory phase (50 ms after target offset), but not during the memory phase (500 ms after target offset). These data support the model hypothesis that the PPC is involved in the attentional selection of a target, whereas the PFC stores saccadic targets during a memory phase.

4.3. Transfer of saccadic adaptation to arm movements

Further experimental support for the model hypothesis of a head map comes from the finding that there is some transfer of saccadic adaptation to arm movements (de Graaf, Pelisson, Prablanc & Goffart, 1995). In these experiments, subjects performed a visually guided saccadic step task with target displacement. The resulting saccadic adaptation was found to significantly modify hand pointing to a target. Both data and model suggest that the target representation for arm movements is body-centered, and that this body-centered representation is built by combining a head-centered target representation with neck information (Guenther, Bullock, Greve & Grossberg, 1994; Brotchie, Andersen, Snyder & Goodman 1995). If, as in our model, saccadic adaptation slowly modifies the head map weights in the PPC, and if this output signal is used in building a body-centered representation, then such saccadic adaptation could affect the representation that is used to control arm movements. Thus, some saccadic learning would transfer to arm movements.

The idea that the representation of space (in the model PPC) is reorganized by target displacement is further supported by the data of Moidell and Bedell (1988). They found that saccadic adaptation modified perceived visual direction in humans by 24% for gain decreases, and 20% for gain increases. This is in the same range of what de Graaf et al. (1995) found for transfer to arm movements (30%) in humans.

4.4. Adaptive differences between monkeys and humans

Is it reasonable to try to apply a single model to both human and monkey data? If the model is correct, then task-specific adaptation is a result of a need to calibrate the inputs to superior colliculus and saccade generator from multiple sources whose distributed activation may depend on task. In humans, a large number of studies have, indeed, found that learning depends on task (Erkelens & Hulleman, 1993; Edelman & Goldberg, 1994; Frens & van Opstal, 1994; Deubel, 1995; Edelman & Goldberg, 1995; Fujita et al., 1995; Fuchs et al.,

1996; Deubel, 1998). In monkey, electrical stimulation studies have suggested that learning in one task does not transfer to other tasks (Fitzgibbon et al., 1986; Edelman & Goldberg, 1995; Melis & Van Gisbergen, 1996), although one study in monkey which did not use electrical stimulation found significant transfer of step task adaptation to other tasks. In particular, Fuchs et al. (1996) found that in monkey, step task adaptation transfers 96% to overlap trials, 88% to memory trials, and 69% to scanning trials, while in humans, Deubel (1998) found 9%, 2%, and 11% adaptation transfer, respectively.

Why might the monkey data show significant transfer, while the human data does not? One possibility is that Fuchs et al. (1996) used too large a target shift (between 30% and 50%), while most human studies use between 25% and 30%. Bridgeman et al. (1975) showed that stimulus movements smaller than 33% are not detectable in humans. Could the monkeys have noticed the target shifts, and then consciously modified their saccades, perhaps believing that an accurate saccade was needed for reward? Fuchs et al. (1996) noted that transfer between tasks for a single monkey was quite variable. For example, in one case, transfer from step adaptation to scanning was 56%, but then they repeated the experiment on same monkey and got 100%. Also, Fuchs et al. (1996) found incomplete transfer between step and scanning (69%), which is far from the 100% expected if there was only one site of learning in the saccadic system.

Another possibility is that the three streams—reactive, attentive, and planned—are less hierarchically organized, or exhibit a different hierarchy, in monkeys than in humans. In our model, if the hierarchy of control was relaxed, for example, allowing the VC/PPC stage to influence saccades in all tasks by reducing the bias toward planned sampling signals in the cerebellar competition, then our model could reproduce the Fuchs et al. (1996) finding of significant transfer. We believe more experimentation is necessary to further investigate the differences between monkey and human with respect to saccadic adaptation.

In all, our elaboration of the SACCART model demonstrates how map and gain learning can cooperate to produce accurate saccades. The model's multiple sources of learning adaptively calibrate the total input to the saccade generator for all task types, resulting in accurate saccades. Computer simulations show that the model's mechanisms can explain the main trends in task-specific adaptation data. Simulations also show that the model can reproduce the finding that adaptation transfer depends on saccade latency. Electrical stimulation of the model can produce vector or goal-directed saccades, depending on which area of the model is stimulated. The model also makes testable predictions about adaptation transfer in cases that have not yet been experimentally studied.

Acknowledgements

G. Gancarz was supported in part by the Defense Advance Projects Agency and the Office of Naval Research (ONR N00014-95-1-0409), the National Science Foundation (NSF IRI-94-01659), and the Office of Naval Research (ONR N00014-92-J-1309, ONR N00014-94-1-0597, and ONR N00014-95-1-0657). S. Grossberg was supported in part by the Defense Advanced Research Projects Agency and the Office of Naval Research (ONR N00014-95-1-0409), the National Science Foundation (NSF IRI-97-20333), and the Office of Naval Research (ONR N00014-92-J-1309 and ONR N00014-95-1-0657). Thanks to Robin Amos and Diana Meyers for their invaluable assistance in the preparation of this manuscript.

Appendix A. Mathematical model description

This section describes the equations and parameters used in simulations of the model. The simulation was one-dimensional, with each layer consisting of a left and right side, with 20 cells (η) per side. The model equations were numerically integrated using a fourth order Runge-Kutta algorithm with a fixed step size of 0.001. Activations were bounded from below at zero. Parameters were chosen to best fit the data. However, the basic model properties are robust to parameter choice.

A.1. Retina

The target position, A , in head-centered coordinates, could vary between 0 (maximally left) and 1 (maximally right). The location, ϑ , on the retina activated by the target depends on the position of the eye in the head, T , where T is the saccade generator's tonic neuron activity, which codes eye position when the eye is not moving:

$$\vartheta = 38[A - T]^+, \quad (2)$$

where $[x]^+$ in Eq. (2) stands for $\max(x, 0)$. The retinal map activity is:

$$R_i = 1 : \text{if } i = \vartheta \text{ while target is on and eye movement is not occurring}$$

$$R_i = 0 : \text{otherwise.} \quad (3)$$

The retinal map activity is cleared during an eye movement in accordance with data on saccadic suppression, which shows that visual function is strongly attenuated during saccades (Shioiri & Cavanagh, 1989; Li & Matin, 1997). This is likely due to the high velocity of saccades, as well as an active mechanism (Lo, 1988; Zhu & Lo, 1996).

A.2. Superior colliculus

The model's superior colliculus is comprised of two cell layers or maps (Grossberg et al., 1997): a peak decay (PD) layer and a spreading wave (SW) layer. The model PD layer represents the SC T cells or burst cells (Munoz & Wurtz, 1995a) which display a fixed peak of activity that decays as the saccade progresses. The model SW layer corresponds to the SC X cells or buildup cells which display a spreading wave of activity (Munoz & Wurtz, 1995b). The most rostral SW cells are called fixation cells since they are active during fixation, and pause during saccades.

A.3. Peak decay at burst cells

The PD layer activities P_i at each position i receive excitatory input from the model retina (R_i), and from the corresponding position in the SW layer (S_i), as in Grossberg et al. (1997). To model the effect of direct electrical stimulation of the SC, the variable β_i represents the excitatory effect of stimulation. The PD layer is inhibited by the model mesencephalic reticular formation (M), by fixation cell activity (S_1), and by the substantia nigra (N_i):

$$\frac{dP_i}{dt} = -20P_i + (1.2 - P_i)(4R_i + 110f(S_i) + \beta_i) - (1 + P_k)(M + 70S_1 + 110n(N_i)). \quad (4)$$

The excitatory input S_i from the SW layer to the PD layer passes through the sigmoidal signal function:

$$f(x) = \frac{x^3}{0.07^3 + x^3}. \quad (5)$$

Nigral inhibition N_i of the PD layer passes through the sigmoidal signal function:

$$n(x) = \frac{x^3}{0.4^3 + x^3}. \quad (6)$$

A.4. Spreading wave at buildup cells

The activities S_i of the SW layer are excited by the retina (R_i), frontal eye field (FEF) input (F_i), visual cortex (VC) input (H_i), the PD layer (P_i), and self-excitatory connections. The term β_i represents the excitatory effects of direct SC electrical stimulation. A unit in the SW layer is inhibited by the mesencephalic reticular formation (M), by the fixation cells (S_1), by the substantia nigra (N_i), and by other SW cells, as in:

$$\frac{dS_i}{dt} = -0.1S_i + (1 - S_i) \times \left[R_i + 4F_i + H_i + 4 \sum_k g([P_k]^+ h_{k-i}) + 40c(S_i) + \beta_i \right]$$

$$-S_i \left[40M + 0.8S_1 + 8n(N_i) + 40 \sum_{k=i-6, k \neq i}^{i+6} c(S_i)m_{k-i} \right], \quad (7)$$

where

$$g(x) = 0.035x^{0.65}, \quad (8)$$

the spread of input from PD to TW is Gaussian:

$$h_{k-j} = 100e^{-0.05(k-j)^2}, \quad (9)$$

the SW feedback signal function equals

$$c(x) = [x - 0.035]^+, \quad (10)$$

and the off-surround kernel is

$$m_{k-j} = e^{-0.02(k-j)^2}. \quad (11)$$

A.5. Fixation cells

The most rostral buildup cells are called fixation cells. Fixation cell activities S_1 receive excitatory input from a fixation signal (ζ), the FEF (F_1), and from the retinal layer (R_1). The fixation cells are inhibited by the burst and buildup cells:

$$\frac{dS_1}{dt} = -0.1S_1 + (0.1 - S_1)(10\zeta + 2F_1 + R_1) - S_1 \left(10 \sum_{j=2}^{\eta} S_j p_j + 10 \sum_{k=2}^{\eta} [P_k]^+ \right), \quad (12)$$

where the fixation signal

$$\zeta = 1 : \text{if } t < \text{time fixation off} \\ \zeta = 0 : \text{otherwise}, \quad (13)$$

and the buildup input kernel equals

$$p_j = 0.1e^{-0.01j^2}. \quad (14)$$

A.6. Mesencephalic reticular formation

The mesencephalic reticular formation is active in Eqs. (4) and (7) if there is activity in the buildup cell layer:

$$M = 1 : \sum_{j=2}^{\eta} S_j > 0 \\ M = 0 : \text{otherwise}. \quad (15)$$

A.7. Substantia nigra

Cell activity N_i in the model substantia nigra is excited by a constant arousal signal and by the fixation signal ζ in Eq. (13). The nigral cells are inhibited by the VC/PPC (H_i) as well as by the FEF (F_i):

$$\frac{dN_i}{dt} = (1 - N_i)(1.7 + 200\zeta) - (N_i + 1)(2n(H_i) + 2n(F_i)). \quad (16)$$

A.8. Visual/parietal cortex

The model's visual/parietal cortex map cell activity (H) is excited by the retina (R). The activity decays rapidly in this map due to the high passive decay rate:

$$\frac{dH_i}{dt} = -0.34H_i + 7(1 - H_i)R_i - H_i \sum_{j \neq i} H_j. \quad (17)$$

The target is transformed from the retinotopic map representation into a head-centered vector representation K (Andersen et al., 1985). This transformation is accomplished in the simplest way possible in our simulations, since it is not the focus of our study. Thus, vector cell activity K is determined by multiplying map activity (H_i) by weights, Z_i , and by adding an eye position signal Ψ . K was held at 0 when there was no target being stored in the retinal map (H). The eye position signal Ψ is set equal to the saccade generator tonic cell activity T when the SC fixation cell activity is greater than 0.05. Thus, during an eye movement, the value of Ψ does not change. In all:

$$K = \sum_{i=1}^n q(H_i)Z_i + \Psi, \quad (18)$$

where

$$q(x) = 1 : \text{if } x > 0.7$$

$$q(x) = 0 : \text{otherwise.} \quad (19)$$

Weights Z_i were learned by using eye position after a saccade as a teaching signal:

$$\frac{dZ_i}{dt} = 10b(H_i)(\Psi - K) \quad (20)$$

where

$$b(x) = \frac{x^5}{0.9^5 + x^5}. \quad (21)$$

The continuous learning gate $b(H_i)$ in Eq. (20) allows some learning even if activity H_i is small.

A.9. Prefrontal cortex

The parietal head-centered vector K is transformed to a head-centered map representation Q in prefrontal cortex (PFC). This transformation is accomplished by using gradients in the connection weights between the vector cells and the map cells, as well as in the thresholds for the cells in the spatial map (Grossberg & Kuperstein, 1986); namely,

$$Q_i = [(K - 0.5)\Lambda_i - \Gamma_i]^+ \quad (22)$$

where weights

$$\Lambda_i = 0.0064i \quad (23)$$

and thresholds

$$\Gamma_i = 0.00008i^2. \quad (24)$$

Both Λ_i and Γ_i are assumed to increase with i , however, Γ_i increases faster-than-linear. This mechanism is illustrated in Fig. 8.

The weight and threshold gradients produce a maximally activated position in the map which varies with the vector cell activation K . The distribution of activity in the map cells Q is illustrated by Fig. 8B. The three oblique solid lines plot $K\Lambda_i$ for three values of K (1, 2, and 3). The faster-than-linear dotted line plots threshold values Γ_i . The activity of a map cell is the difference between a solid and the dotted line. The three vertical lines in the figure denote the peak in the map activity distribution for $K = 1, 2, 3$. Note that for higher vector values K , the location of the peak shifts toward the right.

The map activity is normalized and contrast-enhanced to concentrate all activity at the maximal acti-

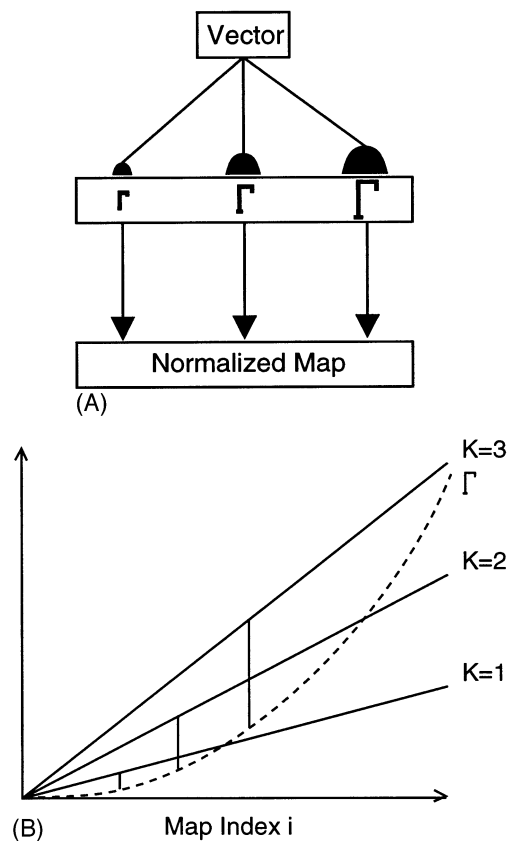


Fig. 8. (A) Vector to map conversion is accomplished using weight (\blacktriangle) and threshold (Γ) gradients. [Figure adapted from Aguilar-Pelaez (1995) with permission.] (B) Solid lines show $K\Lambda_i$ for three values of K , while the dotted line shows threshold values. Map activity is the difference between the solid line and the dotted line. The peak of the map activity for $K = 1, 2, 3$ is plotted by the vertical lines.

vated position by a recurrent on-center, off-surround network (Grossberg, 1973) which chooses a single winning location. The term Ω_i represents direct electrical stimulation of the PFC:

$$\frac{dY_i}{dt} = -0.3Y_i + (1 - Y_i)(15Q_i + 15u(Y_i) + 0.3\Omega_i) - 12Y_i \left(\sum_{k \neq i} u(Y_k) \right) \quad (25)$$

where

$$u(x) = \frac{x^4}{0.8^4 + x^4} \quad (26)$$

A.10. Frontal eye field

The frontal eye field activities, F_i , receive excitatory input from both the visual cortex (H_i) and the prefrontal cortex. Input from the prefrontal cortex is first transformed from the head-centered representation of PFC to the retinotopically-consistent vector representation of the FEF. This transformation is accomplished by first transforming the prefrontal headcentered map representation, Y_i , into a vector, V , by using a weight gradient Π_i , from which an eye position signal (T) is subtracted:

$$V = \left(\sum_{i=1}^n w(Y_i) \Pi_i \right) - T \quad (27)$$

The weight gradient in Eq. (27) was learned. After a target is foveated, the SC fixation cells become activated. This triggers model head-map learning. Learning decreases the difference (error) between the estimate of the head-centered target location V and the final eye position signal T (Grossberg & Kuperstein, 1986). Learning is gated by activity in the prefrontal map Y :

$$\frac{d\Pi_i}{dt} = -80w(Y_i)(V - T) \quad (28)$$

and

$$w(x) = 1 : \text{if } x > 0.5$$

$$w(x) = 0 : \text{otherwise.} \quad (29)$$

The retinotopic vector (V) is then transformed into a retinotopic map (C_i) by using a weight Λ_i and threshold Γ_i gradient; namely,

$$C_i = [V\Lambda_i - \Gamma_i]^+ \quad (30)$$

with weights

$$\Lambda_i = 0.0064i \quad (31)$$

and thresholds

$$\Gamma_i = 0.00008i^2. \quad (32)$$

Map activity (C_i) is then normalized to produce a single peak of activity in map D_i , namely,

$$D_i = \left(\frac{C_i}{\max(C_i) + 0.000001} \right)^{60} \quad (33)$$

Map D excites the frontal eye field map F . Map F also receives excitatory input from visual cortex H . An F map cell is inhibited by other F cells, as well as by the contralateral F map. The FEF is also strongly inhibited by a gating process with activity G , which is modeled here for simplicity as directly influencing FEF but may act in vivo more indirectly, say via basal ganglia gating (Hikosaka & Wurtz, 1985). The gating cell is on until a target is loaded into the PFC:

$$\frac{dF_i}{dt} = -0.02F_i + (1 - F_i)(2y(D) + 3l(H_i) + 2z(F_i)) - F_i \left(4 \sum_{k \neq i} z(F_k) + 8 \sum_{k=1}^n z(F_k^{Contra}) + 40G \right) \quad (34)$$

where

$$y(x) = \frac{x^5}{0.8^5 + x^5} \quad (35)$$

$$l(x) = \frac{x^7}{0.9^7 + x^7} \quad (36)$$

$$z(x) = \frac{x^4}{0.5^4 + x^4} \quad (37)$$

and

$$\frac{dG}{dt} = .3(1 - G) - .42(G + 1) \sum_{k=1}^n a(Y_k) \quad (38)$$

with

$$a(x) = \frac{x^3}{0.5^3 + x^3} \quad (39)$$

A.11. Cerebellum

Each of the three model streams participates in gain learning, which occurs in the model cerebellum. The SC, VC, and FEF each send sampling signals, X , to the cerebellum. These sampling signals represent a pathway's eligibility for learning. The sampling signals compete through mutual inhibition. In all:

$$\frac{dX_i^{sc}}{dt} = -0.1X_i^{sc} + (1 - X_i^{sc})r(P_i) - (X_i^{sc} + 0.05) \left(9.5 \sum_{j=1}^n a(X_j^{vc}) + 6 \sum_{j=1}^n d(X_j^{fef}) \right), \quad (40)$$

$$\frac{dX_i^{vc}}{dt} = -0.1X_i^{vc} + (1 - X_i^{vc})2r(H_i) - (X_i^{vc} + 0.05) \left(12.5 \sum_{j=1}^n e(X_j^{fef}) \right), \quad (41)$$

and

$$\frac{dX_i^{\text{fef}}}{dt} = -0.1X_i^{\text{fef}} + (1 - X_i^{\text{fef}})r(F_i) - (X_i^{\text{fef}} + 0.05) \left(1 \sum_{j=1}^{\eta} o(X_j^{\text{yc}}) \right), \quad (42)$$

where

$$r(x) = \frac{x^4}{0.2^4 + x^4}, \quad (43)$$

$$a(x) = 1 : \text{if } x > 0.75$$

$$a(x) = 0 : \text{otherwise}, \quad (44)$$

$$d(x) = \frac{x^4}{0.6^4 + x^4}, \quad (45)$$

$$e(x) = \frac{x^3}{0.7^3 + x^3}, \quad (46)$$

and

$$o(x) = \frac{x^2}{0.5^2 + x^2}. \quad (47)$$

Learning is triggered in the cerebellum by the teaching signals Y_l (left) and Y_r (right). The onset of a visual target, or the reappearance of a target after a saccade, triggers a teaching signal. The magnitude of the teaching signal depends on the error B , where B is the retinotopic location of the target on the retina. A visual target in the right retina activates the teaching signal:

$$Y_r = 0.45B, \quad (48)$$

and a visual target in the left retina activates the teaching signal:

$$Y_l = 0.45B, \quad (49)$$

The teaching signal is on for one integration step. The adaptive gain weights (W) learn when both the sampling signal X and the teaching signal Y are simultaneously on. Opponent learning allows weights to either increase or decrease and thus correct saccadic undershoots or overshoots (Grossberg & Kuperstein, 1986). The learning rules are given by:

$$\frac{dW_i^{\text{sc}}}{dt} = 150X_i^{\text{sc}}(Y_l - Y_r), \quad (50)$$

$$\frac{dW_i^{\text{ppc}}}{dt} = 80X_i^{\text{ppc}}(Y_l - Y_r), \quad (51)$$

and

$$\frac{dW_i^{\text{fef}}}{dt} = 90X_i^{\text{fef}}(Y_l - Y_r), \quad (52)$$

A.12. Paramedian pontine reticular formation

With planned, attentive, and reactive targets in a common motor-error map representation in the SC, they can compete to select a target position to which the eye will move. For this movement to be accomplished, the target representation is converted from the spatial code of the SC to the temporal code of the oculomotor neurons. This transformation is thought to be accomplished by the saccade-related parts of the reticular formation (Robinson, 1975; Jurgens, Becker & Kornhuber, 1981; Grossberg & Kuperstein, 1986; Scudder, 1988; Gancarz & Grossberg, 1998b). The reticular saccade generator (SG) circuit used in the model is able to quantitatively reproduce saccadic staircases, smooth staircases, interrupted saccades, straight oblique saccades, and saccade velocity saturating after saccade amplitude, among other data properties. For a functional rationale of the SG circuit below, see Gancarz and Grossberg (1998b).

The model SG circuit receives input from the PD and SW layers of the superior colliculus, as well as from the cerebellum. The subscripts l and r refer to the left and right side of the SG, respectively. Only the right side equations are listed, as the left and right side of the model are described by symmetric equations.

The total input to the long-lead burst neuron (LLBN) (right side) of the SG is denoted by I_r and the resultant LLBN activity by L_r . The LLBN receives strong input from the superior colliculus peak decay layer, P , and spreading wave layer, S , and adaptively weighted input from the cerebellum, X , from each of the model's three streams. The LLBN is inhibited by the input I_l to the left side of the SG, and by the right short-lead inhibitory burst neuron (IBN) activity B_r :

$$I_r = 0.2 \sum_{i=1}^{\eta} [4k(S_i) + 4k(P_i) + n(X_i^{\text{sc}})W_i^{\text{sc}} + s(X_i^{\text{ppc}})W_i^{\text{ppc}} + j(X_i^{\text{fef}})W_i^{\text{fef}}] \quad (53)$$

where

$$k(x) = \frac{x^5}{0.1^5 + x^5}, \quad (54)$$

$$s(x) = \frac{x^5}{0.5^5 + x^5}, \quad (55)$$

$$j(x) = \frac{x^3}{0.1^3 + x^3}, \quad (56)$$

and

$$\frac{dL_r}{dt} = -1.3L_r + I_r - 2I_l - 2B_r. \quad (57)$$

The right short-lead excitatory burst neurons (EBN) receive excitatory input from the right LLBNs, as well as an arousal signal (set equal to 1). They are inhibited

by the left LLBNs, as well as by the OPNs via a signal $v(O)$. A model eye movement is considered to be occurring whenever there is greater than zero activity, E_r or E_l , in one or both of the saccade generator EBNs:

$$\frac{dE_r}{dt} = -3.5E_r + 5L_r - 2L_l + 1 - 20v(O). \quad (58)$$

The right inhibitory burst neurons (IBN) are excited by the ipsilateral EBNs and send inhibitory feedback to the ipsilateral LLBNs in Eq. (57):

$$\frac{dB_r}{dt} = -2.4B_r + 3E_r. \quad (59)$$

Omnipause neurons receive excitatory input from an arousal signal (1.2) as well as the SC fixation cells (S_1). They are also inhibited by all the LLBNs:

$$\begin{aligned} \frac{dO}{dt} = & -0.2O + (1 - O)(1.2 + 20S_1) \\ & - 3.5(O + 0.4)(v(L_l) + v(L_r)) \end{aligned} \quad (60)$$

using the signal function:

$$v(x) = \frac{x^4}{0.1^4 + x^4}. \quad (61)$$

Tonic neurons integrate the EBN bursts via a push-pull opponent organization:

$$\frac{dT_r}{dt} = 0.3(E_r - E_l). \quad (62)$$

A.13. Map reset

At the end of a saccade, the SN (N), FEF (F) and VC (H) maps were reset by hand. In vivo an active reset mechanism for regions like FEF may be operative. Such an active reset process has been used to explain other types of cortical data (Carpenter & Grossberg, 1993; Francis, Grossberg & Mingolla, 1994):

$$N_i = 1, \quad (63)$$

$$F_i = 0, \quad (64)$$

and

$$H_i = 0. \quad (65)$$

A.14. Computational details

Target position, timing, and duration as well as other stimulus parameters for the various simulated tasks are as follows. A unit time interval of simulation time was set equal to 50 ms of real world time. Target position (A) of Eq. (2) (in head coordinates) was 0.88 for all adaptation tasks. At the beginning of each trial, the eye was centered in the orbit, and the fixation point (ζ) was on. In adaptation trials, the target location (A) was displaced toward the initial fixation by 0.14 at the end

of the initial saccade. In the simulations of electrical stimulation of the superior colliculus, β_{15} (stimulation strength to SC cell number 15) of Eqs. (4) and (7) was set equal to 200 for the first 100 ms of a trial. Fixation was turned off at time of 25 ms. A visual target was turned on at time 100 ms (during the electrically elicited saccade). In model step trials, the target was turned on at time 25 ms, the same time the fixation point was turned off. In model scanning trials, the target was turned on at time 25 ms, and the fixation point was turned off at time 215 ms, which resulted in saccadic latencies of 305 ms. This latency is comparable to those found experimentally during a scanning task (Deubel, 1995, 1998), and was between the model step latency, and overlap latency. In model overlap trials, the target was turned on at time 25 ms, and the fixation point was turned off at time 400 ms, resulting in overlap times similar to that used in (Deubel, 1995). In the latency effect simulations (Fig. 6B), fixation offset time was varied between time 25 and 775 ms, thus producing a range of saccade latencies over which to compare step to overlap transfer. In calculating saccade latency, an additional 50 ms was added to account for the temporal delay of signals from the retina to visual cortex, not considered in the model. In memory trials, a visible target was flashed for 100 ms (between times 25 and 125ms). The same target flash duration was used in (Deubel, 1995). The fixation point was turned off at time of 300 ms. In the vector saccade simulation (Fig. 7B), model superior colliculus electrical stimulation β_5 (in Eqs. (4) and (7)) was set to 200 for SC cell number 5. In the goal-directed saccade simulation (Fig. 7D), electrical stimulation Ω_1 of the prefrontal cortex (Eq. (25)) was set to 100 for PFC cell number 1.

References

- Aguilar-Pelaez, M.J. (1995). Neural network models of eye movement control, object recognition, and robot navigation. Ph.D. thesis, Boston University.
- Albano, J. E. (1996). Adaptive changes in saccade amplitude: oculocentric or orbitocentric mapping? *Vision Research*, 36, 2087–2098.
- Albus, J. A. (1971). A theory of cerebellar function. *Mathematical Biosciences*, 10, 25–61.
- Andersen, R. A., Essick, G. K., & Siegel, R. M. (1985). Encoding of spatial location by posterior parietal neurons. *Science*, 230, 456–458.
- Anderson, R. A. (1995). Encoding of intention and spatial location in the posterior parietal cortex. *Cerebral Cortex*, 5(5), 457–469.
- Barash, S., Bracewell, M. R., Fogassi, L., Gnadt, J. W., & Andersen, R. A. (1991a). Saccade-related activity in the lateral intraparietal area II. Spatial properties. *Journal of Neurophysiology*, 66(3), 1109–1124.
- Barash, S., Bracewell, M. R., Fogassi, L., Gnadt, J. W., & Andersen, R. A. (1991b). Saccade-related activity in the lateral intraparietal area I. Temporal properties; comparison with area 7a. *Journal of Neurophysiology*, 66(3), 1095–1108.

- Brandt, S. A., Ploner, C. J., Meyer, B.-U., Leistner, S., & Villringer, A. (1998). Effects of repetitive transcranial magnetic stimulation over dorsolateral prefrontal and posterior parietal cortex on memory-guided saccades. *Experimental Brain Research*, *118*, 197–204.
- Bridgeman, B., Hendry, D., & Stark, L. (1975). Failure to detect displacement of the visual world during saccadic eye movements. *Vision Research*, *15*, 719–722.
- Brotchie, P. R., Andersen, R. A., Snyder, L. H., & Goodman, S. J. (1995). Head position signals used by parietal neurons to encode locations of visual stimuli. *Nature*, *375*, 232–235.
- Burman, D. D., & Segraves, M. A. (1994). Primate frontal eye field activity during natural scanning eye movements. *Journal of Neurophysiology*, *71*(3), 1266–1271.
- Carpenter, G., & Grossberg, S. (1993). Normal and amnesic learning, recognition, and memory by a neural model of cortico-hippocampal interactions. *Trends in Neurosciences*, *16*, 131.
- Colby, C. L., Duhamel, J.-R., & Goldberg, M. E. (1995). Oculocentric spatial representation in parietal cortex. *Cerebral Cortex*, *5*(5), 470–481.
- Crandall, W., & Keller, E. (1985). Visual and oculomotor signals in nucleus reticularis tegmenti pontis in alert monkey. *Journal of Neurophysiology*, *54*(5), 1326–1345.
- de Graaf, J. B., Pelisson, D., Prablanc, C., & Goffart, L. (1995). Modifications in end positions of arm movements following short term saccadic adaptation. *NeuroReport*, *6*, 1733–1736.
- Dean, P., Mayhew, J. E., & Langdon, P. (1994). Learning and maintaining saccadic accuracy: a model of brainstem-cerebellar interactions. *Journal of Cognitive Neuroscience*, *6*(2), 117–138.
- Deng, S., Goldberg, M., Segraves, M., & Ungerleider, L. (1986). The effect of unilateral ablation of the frontal eye fields on saccadic performance in the monkey. In E. Keller, & D. Zee, *Adaptive processes in the visual and oculomotor systems* (pp. 201–208). Oxford: Pergamon.
- Deubel, H. (1995). Separate adaptive mechanisms for the control of reactive and volitional saccadic eye movements. *Vision Research*, *35*(23/24), 3529–3540.
- Deubel, H. (1998). Separate mechanisms for the adaptive control of reactive, volitional, and memory-guided saccadic eye movements. In D. Gopher, & A. Koriati, *Attention and performance XVII* (in press).
- Duhamel, J., Colby, C., & Goldberg, M. (1992). The updating of the representation of visual space in parietal cortex by intended eye movements. *Science*, *255*, 90–92.
- Eccles, J. (1979). Introductory remarks. In J. Massion, & K. Sasaki, *Cerebro-cerebellar interactions* (pp. 1–18). Amsterdam: Elsevier.
- Eccles, J., Ito, M., & Szentagothai, J. (1967). *The cerebellum as a neuronal machine*. New York: Springer-Verlag.
- Edelman, J., & Goldberg, M. (1994). Short-term saccadic adaptation occurs at a locus common to the pathways for express and normal-latency saccades. *Society for Neuroscience Abstracts*, *107.2*.
- Edelman, J., & Goldberg, M. (1995). Metrics of saccades evoked by electrical stimulation in the frontal eye fields are not affected by short-term saccadic adaptation. *Society for Neuroscience Abstracts*, *21*, 1195.
- Edelman, J., & Goldberg, M. (1998). Dependence of superior collicular discharge and saccade velocity on visual features at saccade endpoint. *Investigative Ophthalmology and Visual Science*, *39*(4), S458.
- Erkelens, C., & Hulleman, J. (1993). Selective adaptation of internally triggered saccades made to visual targets. *Experimental Brain Research*, *93*, 157–164.
- Fiala, J. C., Grossberg, S., & Bullock, D. (1996). Metabotropic glutamate receptor activation in cerebellar purkinje cells as substrate for adaptive timing of the classically conditioned eye blink response. *Journal of Neuroscience*, *16*, 3760–3774.
- Fischer, B., & Boch, R. (1991). *Cerebral cortex*. In: *Vision and visual dysfunction*, vol. 8 (pp. 277–296). London: Macmillan chp. 12.
- Fitzgibbon, E., Goldberg, M., & Segraves, M. (1986). Short term saccadic adaptation in the monkey. In E. Keller, & D. Zee, *Adaptive processes in visual and oculomotor systems* (pp. 329–333). Oxford: Pergamon.
- Francis, G., Grossberg, S., & Mingolla, E. (1994). Cortical dynamics of feature binding and reset: control of visual persistence. *Vision Research*, *34*(8), 1089–1104.
- Frens, M., & van Opstal, A. (1994). Transfer of short-term adaptation in human saccadic eye movements. *Experimental Brain Research*, *100*, 293–306.
- Fuchs, A. F., Reiner, D., & Pong, M. (1996). Transfer of gain changes from targeting to other types of saccade in the monkey: constraints on possible sites of saccadic gain adaptation. *Journal of Neurophysiology*, *76*(4), 2522–2535.
- Fujita, M. (1982). Adaptive filter model of the cerebellum. *Biological Cybernetics*, *45*, 195–206.
- Fujita, M., Amagai, A., & Minakawa, F. (1995). Adaptation independence of visually guided and memory guided saccades. *Investigative Ophthalmology and Visual Science*, *S354*.
- Fuster, J. (1996). Frontal lobe and the cognitive foundation of behavioral action. In A. Damasio, H. Damasio, & Y. Christen, *Neurobiology of decision-making* (pp. 47–61). New York: Springer.
- Gamlin, P. D., & Clarke, R. J. (1995). Single-unit activity in the primate nucleus reticularis tegmenti pontis related to vergence and ocular accommodation. *Journal of Neurophysiology*, *73*(5), 2115–2119.
- Gancarz, G., & Grossberg, S. (1997). Adaptive saccadic control by superior colliculus, reticular formation, cerebellum, and neocortex. *Society for Neuroscience Abstracts*, *10.6*, 7.
- Gancarz, G., & Grossberg, S. (1998aa). How do multiple learning sites calibrate saccades to reactive, attentive, and planned movement commands? *Investigative Ophthalmology and Visual Science*, *39*(4), S458.
- Gancarz, G., & Grossberg, S. (1998b). A neural model of the saccade generator in the reticular formation. *Neural Networks*, *11*, 1159–1174.
- Goldman-Rakic, P. (1990). Parallel systems in the cerebral cortex: the topography of cognition. In M. Arbib, & J. Robinson, *Natural and artificial parallel computation* (pp. 155–176). Cambridge, MA: MIT chp. 7.
- Goldman-Rakic, P. (1995). Cellular basis of working memory. *Neuron*, *14*, 477–485.
- Grossberg, S. (1969). On learning of spatiotemporal patterns by networks with ordered sensory and motor components. I. Excitatory components of the cerebellum. *Studies in Applied Mathematics*, *48*, 105–132.
- Grossberg, S. (1973). Contour enhancement, short term memory, and constancies in reverberating neural networks. *Studies in Applied Mathematics*, *52*, 213–257.
- Grossberg, S., Guenther, F., Bullock, D., & Greve, D. (1993). Neural representations for sensory-motor control, II: learning a head-centered visuomotor representation of 3-D target position. *Neural Networks*, *6*, 43–67.
- Grossberg, S., & Kuperstein, M. (1986). *Neural dynamics of adaptive sensory-motor control*. Oxford: Pergamon.
- Grossberg, S., & Merrill, J. W. (1996). The hippocampus and cerebellum in adaptively timed learning, recognition, and movement. *Journal of Cognitive Neuroscience*, *8*(3), 257–277.
- Grossberg, S., Roberts, K., Aguilar, M., & Bullock, D. (1997). A neural model of multimodal adaptive saccadic eye movement control by superior colliculus. *Journal of Neuroscience*, *17*(24), 9706–9725.
- Guenther, F. H., Bullock, D., Greve, D., & Grossberg, S. (1994). Neural representations for sensorimotor control. III. Learning a

- body-centered representation of a three-dimensional target position. *Journal of Cognitive Neuroscience*, 6(4), 341–358.
- Hallett, P., & Lightstone, A. (1976). Saccadic eye movements to flashed targets. *Vision Research*, 16, 107–114.
- Henik, A., Rafal, R., & Rhodes, D. (1994). Endogenously generated and visually guided saccades after lesions of the human frontal eye fields. *Journal of Cognitive Neuroscience*, 6(4), 400–411.
- Hikosaka, O., & Wurtz, R. H. (1985). Modification of saccadic eye movements by gaba-related substances. II. Effects of muscimol in monkey substantia nigra pars reticulata. *Journal of Neurophysiology*, 53(1), 292–308.
- Houk, J. C., Buckingham, J. T., & Barto, A. G. (1996). Models of the cerebellum and motor learning. *Behavioral and Brain Sciences*, 19, 368–383.
- Ito, M. (1984). *The cerebellum and neural control*. New York: Raven Chp. 10, 24.
- Jurgens, R., Becker, W., & Kornhuber, H. (1981). Natural and drug-induced variation of velocity and duration of human saccadic eye movements: evidence for control of the neural pulse generator by local feedback. *Biological Cybernetics*, 39, 87–96.
- Karn, K. S., Moller, P., & Hayhoe, M. M. (1997). Reference frames in saccadic targeting. *Experimental Brain Research*, 115, 267–282.
- Keating, E., & Gooley, S. (1988a). Disconnection of parietal and occipital access to the saccadic oculomotor system. *Experimental Brain Research*, 70, 385–398.
- Keating, G. E., & Gooley, S. G. (1988b). Saccadic disorders caused by cooling the superior colliculus or the frontal eye field, or from combined lesions of both structures. *Brain Research*, 438, 247–255.
- Kurylo, D. D., & Skavenski, A. A. (1991). Eye movements elicited by electrical stimulation of area pg in the monkey. *Journal of Neurophysiology*, 65(6), 1243–1253.
- Lee, K., & Tehovnik, E. J. (1995). Topographic distribution of fixation-related units in the dorsomedial frontal cortex of the rhesus monkey. *European Journal of Neuroscience*, 7, 1005–1011.
- Li, W., & Martin, L. (1997). Saccadic suppression of displacement: separate influences of saccade size and of target retinal eccentricity. *Vision Research*, 37(13), 1779–1797.
- Lo, F. (1988). A study of neuronal circuitry mediating the saccadic suppression in the rabbit. *Experimental Brain Research*, 71(3), 618–622.
- Lynch, J. C. (1992). Saccade initiation and latency deficits after combined lesions of the frontal and posterior eye fields in monkeys. *Journal of Neurophysiology*, 68(5), 1913–1916.
- Mann, S., Thau, R., & Schiller, P. (1988). Conditional task-related responses in monkey dorsomedial frontal cortex. *Experimental Brain Research*, 69, 460–468.
- Marr, D. (1969). A theory of cerebellar cortex. *Journal of Physiology (London)*, 202, 437–470.
- Mays, L., & Sparks, D. (1980). Saccades are spatially, not retinocentrically, coded. *Science*, 1163–1165.
- McLaughlin, S. (1967). Parametric adjustment in saccadic eye movements. *Perception and Psychophysics*, 2, 359–362.
- Melis, B. J., & Van Gisbergen, J. A. (1996). Short-term adaptation of electrically induced saccades in monkey superior colliculus. *Journal of Neurophysiology*, 76(3), 1744–1758.
- Meredith, A. M., & Stein, B. E. (1986). Visual, auditory, and somatosensory convergence on cells in superior colliculus results in multisensory integration. *Journal of Neurophysiology*, 56(3), 640–662.
- Moidell, B. G., & Bedell, H. E. (1988). Changes in oculocentric visual direction induced by the recalibration of saccades. *Vision Research*, 28(2), 329–336.
- Mountcastle, V., Anderson, R., & Motter, B. (1981). The influence of attentive fixation upon the excitability of the light-sensitive neurons of the posterior parietal cortex. *Journal of Neuroscience*, 1, 1218–1235.
- Munoz, D. P., Waitzman, D. M., & Wurtz, R. H. (1996). Activity of neurons in monkey superior colliculus during interrupted saccades. *Journal of Neurophysiology*, 75(6), 2562–2580.
- Munoz, D. P., & Wurtz, R. H. (1995a). Saccade-related activity in monkey superior colliculus I. Characteristics of burst and buildup cells. *Journal of Neurophysiology*, 73(6), 2313–2333.
- Munoz, D. P., & Wurtz, R. H. (1995b). Saccade-related activity in monkey superior colliculus II. Spread of activity during saccades. *Journal of Neurophysiology*, 73(6), 2334–2348.
- Noda, H., Sugita, S., & Ikeda, Y. (1990). Afferent and efferent connections of the oculomotor region of the fastigial nucleus in the macaque monkey. *Journal of Comparative Neurology*, 302, 330–348.
- Ojakangas, C., & Ebner, T. (1992). Transient cerebellar climbing fiber activity during motor learning: relationship to kinematics. *Society for Neuroscience Abstracts*, 178.4, 406.
- Perrett, S. P., Ruiz, B. P., & Mauk, M. D. (1993). Cerebellar cortex lesions disrupt learning-dependent timing of conditioned eyelid responses. *Journal of Neuroscience*, 13(4), 1708–1718.
- Posner, M. I., Walker, J. A., Friedrich, F. A., & Rafal, R. D. (1987). How do the parietal lobes direct covert attention. *Neuropsychologia*, 25(1A), 135–145.
- Raybourn, M. S., & Keller, E. L. (1977). Colliculoreticular organization in primate oculomotor system. *Journal of Neurophysiology*, 40(4), 861–878.
- Robinson, D. (1975). Oculomotor control signals. In G. Lennerstrand, & P. Bach-y Rita, *Basic mechanisms of ocular motility and their clinical implications*. Oxford: Pergamon.
- Robinson, D., & Fuchs, A. (1969). Eye movements evoked by stimulation of frontal eye fields. *Journal of Neurophysiology*, 32, 637–648.
- Robinson, D. L., Bushnell, C. M., & Goldberg, M. E. (1981). Role of posterior parietal cortex in selective visual attention. In Fuchs, & Becker, *Progress in oculomotor research*. Amsterdam: Elsevier.
- Schall, J., Morel, A., King, D., & Bullier, J. (1995). Topography of visual cortex connections with frontal eye field in macaque: convergence and segregation of processing streams. *Journal of Neuroscience*, 15, 4464–4487.
- Schall, J. D. (1991). Neural basis of saccadic eye movements in primates. In *Vision and visual dysfunction* (pp. 388–442). chp. 15.
- Schiller, P. H., True, S. D., & Conway, J. L. (1979). Paired stimulation of the frontal eye fields and the superior colliculus of the rhesus monkey. *Brain Research*, 179, 162–164.
- Schiller, P., & Sandell, J. (1983). Interactions between visually and electrically elicited saccades before and after superior colliculus and frontal eye field ablations in the rhesus monkey. *Experimental Brain Research*, 49, 381–392.
- Schiller, P., & Stryker, M. (1972). Single-unit recording and stimulation in superior colliculus of the alert rhesus monkey. *Journal of Neurophysiology*, 35, 915–924.
- Schlag-Rey, M., Schlag, J., & Dassonville, P. (1992). How the frontal eye field can impose a saccade goal on superior colliculus neurons. *Journal of Neurophysiology*, 67(4), 1003–1005.
- Schnyder, H., Reisine, H., Hepp, K., & Henn, V. (1985). Frontal eye field projection to the paramedian pontine reticular formation traced with wheat germ agglutinin in the monkey. *Brain Research*, 329, 151–160.
- Scudder, C. A. (1988). A new local feedback model of the saccadic burst generator. *Journal of Neurophysiology*, 59(5), 1455–1475.
- Segraves, M. A. (1992). Activity of monkey frontal eye field neurons projecting to oculomotor regions of the pons. *Journal of Neurophysiology*, 68(6), 1967–1985.
- Segraves, M. A., & Park, K. (1993). The relationship of monkey frontal eye field activity to saccade dynamics. *Journal of Neurophysiology*, 69(6), 1880–1889.
- Shioiri, S., & Cavanagh, P. (1989). Saccadic suppression of low-level motion. *Vision Research*, 29(8), 915–928.

- Stanford, T. R., Freedman, E. G., & Sparks, D. L. (1996). Site and parameters of microstimulation: evidence for independent effects on the properties of saccades evoked from the primate superior colliculus. *Journal of Neurophysiology*, *76*(5), 3360–3381.
- Steinmetz, M., & Constantinidis, C. (1995). Neurophysiological evidence for a role of posterior parietal cortex in redirecting visual attention. *Cerebral Cortex*, *5*(5), 448–456.
- Stricanne, B., Andersen, R. A., & Mazzoni, P. (1996). Eye-centered, head-centered, and intermediate coding of remembered sound locations in area LIP. *Journal of Neurophysiology*, *76*(3), 2071–2076.
- Tehovnik, E. J., Lee, K., & Schiller, P. H. (1994). Stimulation-evoked saccades from the dorsomedial frontal cortex of the rhesus monkey following lesions of the frontal eye fields and superior colliculus. *Experimental Brain Research*, *98*, 179–190.
- Thielert, C., & Thier, P. (1993). Patterns of projections from the pontine nuclei and the nucleus reticularis tegmenti pontis to the posterior vermis in the rhesus monkey: a study using retrograde tracers. *Journal of Comparative Neurology*, *337*(1), 113–126.
- White, J. M., Sparks, D. L., & Stanford, T. R. (1994). Saccades to remembered target locations: an analysis of systematic and variable errors. *Vision Research*, *34*(1), 79–92.
- Wilson, F. A., Ó Scalaidhe, S. P., & Goldman-Rakic, P. S. (1993). Dissociation of object and spatial processing domains in primate prefrontal cortex. *Science*, *260*, 1955–1958.
- Wolf, W., Deubel, H., & Hauske, G. (1984). Properties of parametric adjustment in the saccadic system. In A. Gale, & F. Johnson, *Theoretical and applied aspects of eye movement research* (pp. 79–86). Amsterdam: Elsevier.
- Zhu, J., & Lo, F. (1996). Time course of inhibition induced by a putative saccadic suppression circuit in the dorsal lateral geniculate nucleus of the rabbit. *Brain Research Bulletin*, *41*(5), 281–291.
- Zingale, C., & Kowler, E. (1987). Planning sequences of saccades. *Vision Research*, *27*, 1327–1341.
- Zipser, D., & Andersen, R. A. (1988). A back-propagation programmed network that simulates response properties of a subset of posterior parietal neurons. *Nature*, *331*, 679–684.